

**Kaimieva O. S.<sup>1</sup>, Danilova V. V.<sup>1</sup>, Buyanova E. S.<sup>1</sup>,  
Petrova S. A.<sup>2</sup>, Nikolaenko I. V.<sup>1,3</sup>**

<sup>1</sup>*Institute of Natural Sciences and Mathematics,  
Ural Federal University,  
19 Mira St., 620002, Ekaterinburg,  
Russian Federation*

<sup>2</sup>*Institute of Metallurgy,  
Ural Branch of Academy of Sciences,  
101 Amundsena st., 620016, Ekaterinburg, Russian Federation*

<sup>3</sup>*Institute of Solid State Chemistry,  
Ural Branch of Academy of Sciences,  
91 Pervomayskaya St., Ekaterinburg, 620049, Russian Federation  
kaimi-olga@mail.ru*

## Thermodynamic database for multicomponent oxide systems. Preparation, Structure and Physicochemical Properties of $\text{La}_{0.95}\text{Bi}_{0.05}\text{Mn}_{1-y}\text{Cu}_y\text{O}_{3+6}$ ( $y = 0.1 - 0.4$ ) and Composites with $\text{Bi}_2\text{O}_3$ -Based Electrolytes

Samples of  $\text{La}_{0.95}\text{Bi}_{0.05}\text{Mn}_{1-y}\text{Cu}_y\text{O}_{3+6}$  ( $y = 0.1 - 0.4$ ) were prepared by solid-state synthesis. Additionally, the sample with nominal composition  $\text{La}_{0.95}\text{Bi}_{0.05}\text{Mn}_{0.7}\text{Cu}_{0.3}\text{O}_{3+6}$  was obtained using citrate-nitrate method. It was determined by X-ray diffraction analysis that the compounds have rhombohedral (space group  $R\bar{3}C$ ) or orthorhombic (space group  $Pbnm$ ) structure, depending on the composition. Single-phase compounds are synthesized at  $y = 0.1$ ;  $0.2$ . The investigation using scanning electron microscope showed that the grain sizes for the samples sintered using different techniques are close to each other because of the high calcination temperature. For the sample with orthorhombic structure the phase transition into rhombohedral one was found around  $390^\circ\text{C}$  by means of dilatometry. Thermal expansion coefficient of the sample  $\text{La}_{0.95}\text{Bi}_{0.05}\text{Mn}_{0.7}\text{Cu}_{0.3}\text{O}_{3+6}$  is equal to  $6 \cdot 10^{-6} \text{K}^{-1}$  ( $T < 390^\circ\text{C}$ ) and  $15 \cdot 10^{-6} \text{K}^{-1}$  ( $T > 390^\circ\text{C}$ ). The composite materials of substituted lanthanum manganites with  $\text{Bi}_4\text{V}_{1.7}\text{Fe}_{0.5}\text{O}_{11-5}$  and  $\text{Bi}_7\text{Nb}_{1.8}\text{Zr}_{0.2}\text{O}_{15.5-6}$  solid electrolytes were obtained at  $650^\circ\text{C}$ . The electrical conductivity values for the latter one are by three orders of magnitude higher than for pure bismuth niobate.

**Keywords:** lanthanum manganite, perovskite-like structure, mixed conductor, composite

Received: 02.06.2018. Accepted: 19.07.2018. Published: 30.07.2018.

© Kaimieva O. S., Danilova V. V., Buyanova E. S., Petrova S. A., Nikolaenko I. V., 2018

### Introduction

The search for new catalysts and electrode materials for solid oxide fuel cells, aimed to replace expensive platinum, is an important issue in modern materials chemistry. Perovskite-type compound  $\text{LaMnO}_3$  is of particular interest in this area. Lanthanum

num manganite has sufficiently high values of mixed conductivity ( $\sim 80$  S/cm [1]) with thermal expansion coefficient (TEC) value equal to  $10.7 \times 10^{-6} \text{ K}^{-1}$  [2]. On the one hand, authors [3–5] showed that doping of lanthanum manganite by  $\text{Cu}^{2+}$  ions improves its electroconductive characteristics comparing with such dopants as Fe, Ni, Co, Cr, Zn. However, the homogeneity range of the solid solution  $\text{LaMn}_{1-x}\text{Cu}_x\text{O}_{3+\delta}$  has not yet been determined exactly. Some authors suppose that single-phase compounds are formed at  $x \leq 0.6$  [6–8]. But in the other cases, this value is equal to 0.8 [9] and 0.4 [10]. Outside the homogeneity range, many authors [6–10] report existence of such impurities as  $\text{La}_2\text{CuO}_4$  and  $\text{CuO}$ . On the other hand, it was shown that preparation of composite materials containing lanthanum manganite and oxygen-ion conductor improved the performance of an electrochemical cell because of the extension of the triple-phase boundary region from the electrolyte/electrode physical interface into the electrode bulk [11, 12]. For example, the composite electrode ( $(\text{La}_{0.85}\text{Sr}_{0.15})_{0.9}\text{MnO}_{3-\delta}$  and  $(\text{Y}_{0.25}\text{Bi}_{0.75})_2\text{O}_3$ )

## Experimental

Samples  $\text{La}_{0.95}\text{Bi}_{0.05}\text{Mn}_{1-y}\text{Cu}_y\text{O}_{3+\delta}$  ( $y=0.1-0.4$ ) were prepared via the solid-state method. Additionally, the sample  $\text{La}_{0.95}\text{Bi}_{0.05}\text{Mn}_{0.7}\text{Cu}_{0.3}\text{O}_{3+\delta}$  was synthesized using citrate-nitrate method to study the influence of synthesis method on the structure. Metal oxides  $\text{Bi}_2\text{O}_3$  (99.99%),  $\text{La}_2\text{O}_3$  (La-D),  $\text{MnO}_2$  (98%),  $\text{CuO}$  (99.9%) were taken as precursors. For accurate weighing, all oxides had been annealed in air at different temperatures for removing water and obtaining the stable modifications. For  $\text{Bi}_2\text{O}_3$ , the annealing temperature was equal to  $600^\circ\text{C}$ ,  $\text{La}_2\text{O}_3$ – $1000^\circ\text{C}$ ,  $\text{MnO}_2$ – $750^\circ\text{C}$ ,  $\text{CuO}$  –  $600^\circ\text{C}$ . Manganese (IV) oxide was

showed much lower polarization resistance values than composites with yttrium-stabilized zirconia [13]. In our previous works [14, 15] it was observed that the solid solution  $\text{La}_{1-x}\text{Bi}_x\text{Mn}_{1-y}\text{Cu}_y\text{O}_{3+\delta}$ , simultaneously doped with Bi and Cu, can be obtained by solid-state method within limited homogeneity range ( $x, y \leq 0.1$ ). The chemical compatibility of these compounds as cathode materials was tested with some solid electrolytes ( $\text{Bi}_4\text{V}_{1.7}\text{Fe}_{0.3}\text{O}_{11-\delta}$  and  $\text{La}_{0.9}\text{Bi}_{0.1}\text{Nb}_{0.9}\text{W}_{0.1}\text{O}_{3+\delta}$ ). The results of X-ray diffraction analysis confirmed that the materials investigated do not interact at temperatures lower than  $700^\circ\text{C}$  [15]. But a detailed study of structure of  $\text{La}_{1-x}\text{Bi}_x\text{Mn}_{1-y}\text{Cu}_y\text{O}_{3+\delta}$  and electrochemical behavior of composites has not been presented.

Therefore, the aim of our work is to obtain the samples with general formula  $\text{La}_{1-x}\text{Bi}_x\text{Mn}_{1-y}\text{Cu}_y\text{O}_{3+\delta}$  ( $x=0.05, y=0.1-0.4$ ) by solid-state and citrate-nitrate methods and to study the physicochemical properties of synthesized compounds and its composites with  $\text{Bi}_4\text{V}_{1.7}\text{Fe}_{0.3}\text{O}_{11-\delta}$  and  $\text{Bi}_7\text{Nb}_{1.8}\text{Zr}_{0.2}\text{O}_{15.5-\delta}$ .

reduced to  $\text{Mn}_2\text{O}_3$  in the process. Lanthanum oxide was weighted shortly after annealing. Solid-state synthesis was performed by regrinding of the oxide mixture thoroughly in an agate mortar using ethanol as a homogenizer. The multi-step synthesis was carried out in the temperature range  $600$ – $1270^\circ\text{C}$ . Annealing time was 8 hour at each stage. After annealing of powder samples at  $700^\circ\text{C}$ , they were uniaxially pressed into rectangular bars and then sintered at  $1200^\circ\text{C}$ .

For citrate-nitrate method, initial oxides were dissolved into deionized water by adding nitric acid. Full dissolution

of manganese oxide was achieved by adding oxalic acid. Then as-prepared solutions were mixed with citric acid (in the molar ratio 1 (number of metal atoms in lanthanum manganite): 2 (citric acid)) in a ceramic bowl and heated until self-combustion occurred. After that, as-obtained powder was annealed at 600 °C, and then at 900–1200 °C.

The phase composition of the powders was checked by means of X-ray powder diffraction (D8 ADVANCE diffractometer (Bruker, Germany), Cu K $\alpha$  radiation,  $\beta$ -filter, PSD V $\ddot{A}$ NTEC1. The phase purity of the compounds was examined by comparing their XRD patterns with those in the PDF2 database. Crystal structure refinements were performed using full-profile Rietveld method. The oxygen nonstoichiometry ( $\delta$ ) was determined by redox potentiometric titration (automatic potentiometric titrator ATP-2 AKVILON) at room temperature [16]. A surface morphology and a local chemical composition of the powder and ceramic specimens fired at 1200–1270 °C were determined using scanning electron microscopy (SEM) on microscope JEOL JSM 6390LA (Jeol, Japan). The density of sintered briquettes was estimated with Archimedes method. Dilatometric measu-

rements were carried out on rectangular bars with the length of 25 mm using a DIL 402 C Netzsch dilatometer in the temperature range 20–1000 °C with a heating rate of 2 °C/min. For electrical conductivity measurements, composite materials were prepared with bismuth-containing electrolytes Bi<sub>4</sub>V<sub>1.7</sub>Fe<sub>0.3</sub>O<sub>11- $\delta$</sub>  (BIFEVOX0.3) and Bi<sub>7</sub>Nb<sub>1.8</sub>Zr<sub>0.2</sub>O<sub>15.5- $\delta$</sub>  (BNZO0.2) [15]. The composition La<sub>0.95</sub>Bi<sub>0.05</sub>Mn<sub>0.8</sub>Cu<sub>0.2</sub>O<sub>3+ $\delta$</sub>  + BIFEVOX0.3 (1:1 wt. %) is referred to as “Composite1” and the other one La<sub>0.95</sub>Bi<sub>0.05</sub>Mn<sub>0.6</sub>Cu<sub>0.4</sub>O<sub>3+ $\delta$</sub>  + BNZO0.2 (1:1 wt. %) – “Composite2”. These materials were sintered at 650 °C where there is no chemical interaction between the powders [15]. All samples were coated by highly disperse platinum before measurements. Electrical conductivity was measured with impedance spectroscopy (impedance meter Z-3000 “Elins”, Russia) using two-probe cell. The measurements were performed in the temperature range 650–200 °C and frequency span 3 MHz – 1 Hz in the cooling mode. Obtained impedance spectra were treated with “ZView” software and equivalent circuits were fitted to them. Using these data, the temperature dependences of electrical conductivity ( $\sigma$ ) were plotted in Arrhenius coordinates  $\lg \sigma - 1000/T$ .

## Results and discussion

It was determined by X-ray diffraction analysis that the compounds La<sub>0.95</sub>Bi<sub>0.05</sub>Mn<sub>1- $y$</sub> Cu <sub>$y$</sub> O<sub>3+ $\delta$</sub>  at  $y = 0.1; 0.2$  are single-phase and have rhombohedral (space group  $R\bar{3}c$ ) structure. But with an increase in copper doping level the structure changes to orthorhombic one (space group  $Pbnm$ ) with the simultaneous appearance of impurity phase CuO (5–10 wt. %). The samples La<sub>0.95</sub>Bi<sub>0.05</sub>Mn<sub>0.7</sub>Cu<sub>0.3</sub>O<sub>3+ $\delta$</sub>  obtained by different sintering methods have identi-

cal structure and impurity. X-ray diffraction pattern of the La<sub>0.95</sub>Bi<sub>0.05</sub>Mn<sub>0.8</sub>Cu<sub>0.2</sub>O<sub>3+ $\delta$</sub>  is given in Fig. 1. The refinement results performed by Rietveld method are listed in Table 1.

The value of oxygen nonstoichiometry determined by redox titration method at room temperature for the single-phase specimens La<sub>0.95</sub>Bi<sub>0.05</sub>Mn<sub>1- $y$</sub> Cu <sub>$y$</sub> O<sub>3+ $\delta$</sub>  ( $y = 0.1; 0.2$ ) is equal to 0.12. Using scanning electron microscopy, we compared

powder particles” size for the samples of  $\text{La}_{0.95}\text{Bi}_{0.05}\text{Mn}_{0.7}\text{Cu}_{0.3}\text{O}_{3+\delta}$  synthesized via the solid-state and citrate-nitrate methods.

The images are shown in the Fig. 2. It was found there is no significant influence of the sintering method on the grains size of the powder sample. It can be explained by high calcination temperature (1200 °C) of the substituted lanthanum manganite prepared by citrate-nitrate technique. As seen in Fig. 2, powder particles have vari-

ous shapes with size distribution from 5 to 50  $\mu\text{m}$ .

For the dilatometric and electrical conductivity measurements, substituted lanthanum manganites or composite samples (electrode and electrolyte mixture) were pressed and sintered into bars. Volumetric porosity of  $\text{La}_{0.95}\text{Bi}_{0.05}\text{Mn}_{1-y}\text{Cu}_y\text{O}_{3+\delta}$  ( $y = 0.1 - 0.4$ ) ceramics obtained at 1200 °C was estimated by Archimedes method. The average value of 14% was additionally

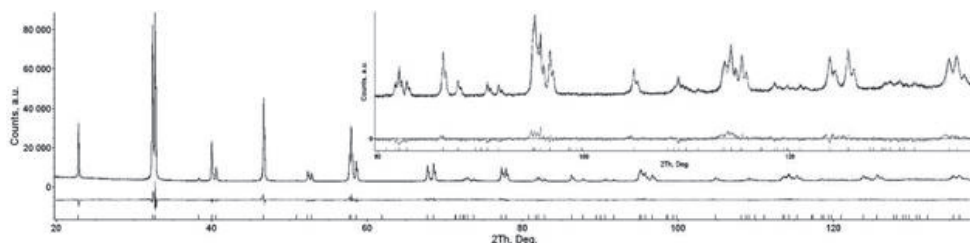


Fig. 1. X-ray diffraction pattern of the  $\text{La}_{0.95}\text{Bi}_{0.05}\text{Mn}_{0.8}\text{Cu}_{0.2}\text{O}_{3+\delta}$ . Inset: the extended scale of large angles (80–130°)

Table 1

The refinement results for the  $\text{La}_{0.95}\text{Bi}_{0.05}\text{Mn}_{0.8}\text{Cu}_{0.2}\text{O}_{3+\delta}$

Composition		$\text{La}_{0.95}\text{Bi}_{0.05}\text{Mn}_{0.8}\text{Cu}_{0.2}\text{O}_{3+\delta}$				
Space group		$R\bar{3}c$				
Unit cell parameter, $a$ (Å)		5.5269(1)				
Unit cell parameter, $c$ (Å)		13.3356(1)				
Volume (Å <sup>3</sup> )		352.784(5)				
GOF		2.86				
$R_{\text{exp}}$		1.55				
$R_{\text{wp}}$		4.43				
$R_{\text{p}}$		3.17				
$R_{\text{Bragg}}$		2.94				
Atom	Multiplicity	$x$	$y$	$z$	Occupation	Beq.
La	6	0.00000	0.00000	0.25000	0.952 (1)	0.34
Bi	6	0.00000	0.00000	0.25000	0.048 (2)	0.34
Mn	6	0.00000	0.00000	0.00000	0.80 (1)	0.10
Cu	6	0.00000	0.00000	0.00000	0.20 (1)	0.10
O	18	0.5490 (7)	0.00000	0.25000	1	0.49

confirmed by SEM images of the  $\text{La}_{0.95}\text{Bi}_{0.05}\text{Mn}_{0.7}\text{Cu}_{0.3}\text{O}_{3+\delta}$  tablet (Fig. 3). This value conforms to the general requirements for cathode materials [17]. However, for this sample, the phase transition from orthorhombic to rhombohedral structure is observed at 390 °C (Fig. 4). Thermal expansion coefficient (TEC) value is equal to  $6 \cdot 10^{-6} \text{ K}^{-1}$  ( $T < 390 \text{ °C}$ ) and  $15 \cdot 10^{-6} \text{ K}^{-1}$  ( $T > 390 \text{ °C}$ ).

The electrical conductivity was investigated on composite materials  $\text{La}_{0.95}\text{Bi}_{0.05}\text{Mn}_{0.8}\text{Cu}_{0.2}\text{O}_{3+\delta} + \text{Bi}_4\text{V}_{1.7}\text{Fe}_{0.3}\text{O}_{11-\delta}$  (1:1 wt. %) and  $\text{La}_{0.95}\text{Bi}_{0.05}\text{Mn}_{0.6}\text{Cu}_{0.4}\text{O}_{3\pm\delta} + \text{Bi}_7\text{Nb}_{1.8}\text{Zr}_{0.2}\text{O}_{15.5}$  (1:1 wt. %) using impedance spectroscopy method in temperature range 650–200 °C. As an example,

typical impedance spectrum of the  $\text{La}_{0.95}\text{Bi}_{0.05}\text{Mn}_{0.8}\text{Cu}_{0.2}\text{O}_{3+\delta} + \text{Bi}_4\text{V}_{1.7}\text{Fe}_{0.3}\text{O}_{11-\delta}$  at low temperature (350 °C) is shown in Figure 5. It can be described by resistance ( $R_1$ ) of the sample and the diffusive Warburg ( $W_1$ ) element connected in series. Additionally, constant phase element (CPE1) is in a parallel to  $R_1$  (Fig. 5) and can describe a wide range of electrochemical processes. The value of CPE1 is equal to  $2.5 \times 10^{-4} \text{ F}$  and corresponds to a resistance of phase boundary. Such result is in a good agreement with the composite nature of the material [18].

According to results of a resistance measurements, the temperature dependences of the general electrical conductivity

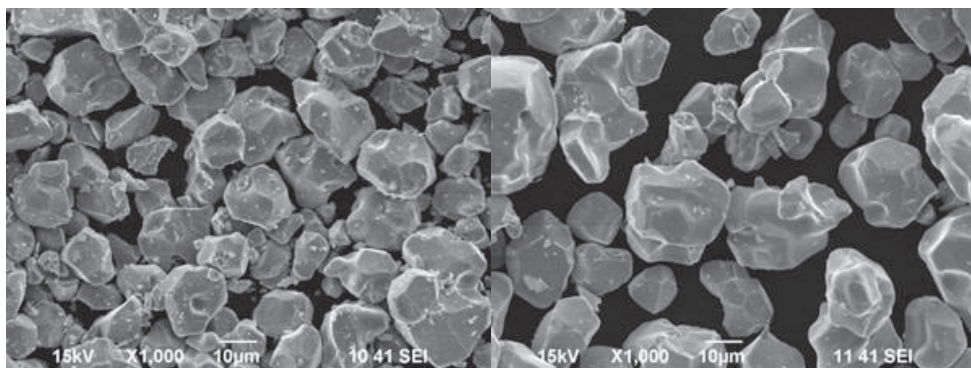


Fig. 2. SEM images of the powder sample  $\text{La}_{0.95}\text{Bi}_{0.05}\text{Mn}_{0.7}\text{Cu}_{0.3}\text{O}_{3+\delta}$ : solid-state method (left); citrate-nitrate method (right)

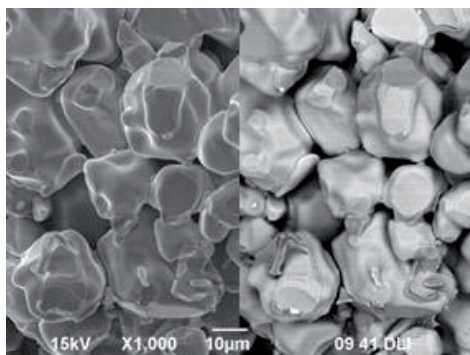


Fig. 3. SEM image of the  $\text{La}_{0.95}\text{Bi}_{0.05}\text{Mn}_{0.7}\text{Cu}_{0.3}\text{O}_{3+\delta}$  tablet chip obtained in secondary (left) and reflected (right) electrons

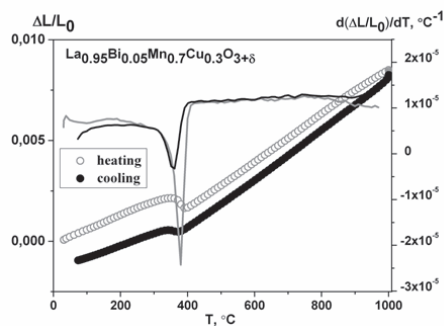


Fig. 4. Temperature dependence of linear thermal expansion and TEC for the sample  $\text{La}_{0.95}\text{Bi}_{0.05}\text{Mn}_{0.7}\text{Cu}_{0.3}\text{O}_{3+\delta}$



ity were plotted for electrochemical cells with: 1) pure electrolyte BIFEVOX0.3 with platinum and composite electrodes; 2) pure electrolyte BNZO0.2 with platinum electrodes; 3) composites with platinum electrodes (Fig. 6). In the case of BIFEVOX0.3, we found out that using the composite materials had the negative influence on the electrical conductivity of the cells. But it can be mentioned that the activation energy ( $E_a$ ) values change insignificantly (Table 2).

Better results were achieved using the composite which contained BNZO0.2,

## Conclusions

Samples with general formula  $\text{La}_{0.95}\text{Bi}_{0.05}\text{Mn}_{1-y}\text{Cu}_y\text{O}_{3+\delta}$  ( $y=0.1-0.4$ ) were prepared by solid-state synthesis. Additionally, the sample with nominal composition  $\text{La}_{0.95}\text{Bi}_{0.05}\text{Mn}_{0.7}\text{Cu}_{0.3}\text{O}_{3+\delta}$  was ob-

where the electrical conductivity values increased by three orders of magnitude at low temperature (300 °C) in comparison with pure bismuth niobate (Fig. 6). Moreover, the activation energy value decreased from 1.10 to 0.32 eV (Table 2), implying considerable contribution of electronic component to the total electrical conductivity of the composite. We suppose that difference in electrochemical behavior of the composite materials investigated is largely determined by structural characteristics and charge transfer of the pure electrolytes.

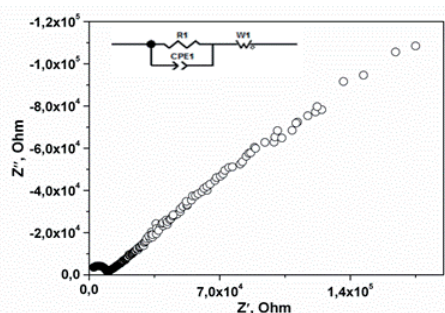


Fig. 5. Impedance spectrum of the Composite1 ( $\text{La}_{0.95}\text{Bi}_{0.05}\text{Mn}_{0.8}\text{Cu}_{0.2}\text{O}_{3+\delta}$  +  $\text{Bi}_4\text{V}_{1.7}\text{Fe}_{0.3}\text{O}_{11-\delta}$  (1:1 wt. %)) at 350 °C and fitted equivalent circuit

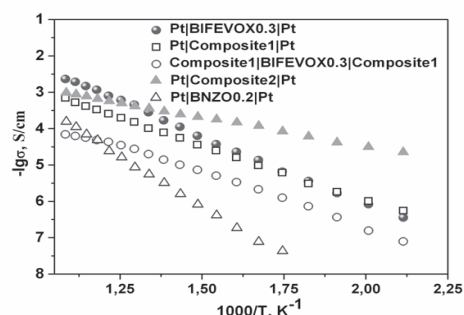


Fig. 6. Temperature dependences of the general electrical conductivity of the investigated electrochemical cells

Table 2  
Electrical conductivity ( $\sigma$ ) and activation energy ( $E_a$ ) values of the electrochemical cells

Electrochemical cell	$\sigma$ , S/cm		$E_a$ , eV
	350 °C	650 °C	
Pt BNZO0.2 Pt	$1.9 \times 10^{-7}$	$1.57 \times 10^{-4}$	1.10
Pt Composite2 Pt	$1.49 \times 10^{-4}$	$9.80 \times 10^{-4}$	0.32
Composite1 BIFEVOX0.3 Composite1	$3.40 \times 10^{-6}$	$6.96 \times 10^{-5}$	0.59
Pt Composite1 Pt	$1.30 \times 10^{-5}$	$6.98 \times 10^{-4}$	0.62
Pt BIFEVOX0.3 Pt	$2.30 \times 10^{-5}$	$2.32 \times 10^{-3}$	0.74

composition. Single-phase compounds are formed at  $y=0.1$ ;  $0.2$ . The investigation using scanning electron microscope showed that samples sintered using different techniques have similar grain sizes because of the high calcination temperature. The average density value estimated by Archimedes method was 14%. For the sample with orthorhombic structure the phase transition into rhombohedral one was found around  $390\text{ }^{\circ}\text{C}$  by dilatometric method. Thermal expansion coefficient of the

sample  $\text{La}_{0.95}\text{Bi}_{0.05}\text{Mn}_{0.7}\text{Cu}_{0.3}\text{O}_{3+\delta}$  is equal to  $6\cdot 10^{-6}\text{ K}^{-1}$  ( $T < 390\text{ }^{\circ}\text{C}$ ) and  $15\cdot 10^{-6}\text{ K}^{-1}$  ( $T > 390\text{ }^{\circ}\text{C}$ ). The composite materials with  $\text{Bi}_4\text{V}_{1.7}\text{Fe}_{0.3}\text{O}_{11-\delta}$  and  $\text{Bi}_7\text{Nb}_{1.8}\text{Zr}_{0.2}\text{O}_{15.5-\delta}$  solid electrolytes were investigated. The electrical conductivity values for the latter were found to be three orders of magnitude higher than those for pure bismuth niobate. However, on the other hand, we found out that using the composites materials with bismuth vanadate had the negative influence on the electrical conductivity of the cells.

### Acknowledgements

The work was carried out within the framework of the state task of the Ministry of education and science of the Russian Federation № 4.2288.2017/PCh.

### References

1. Kuo JH, Anderson HU, Sparlin DM. Oxidation-reduction behavior of undoped and Sr-doped  $\text{LaMnO}_3$ . Defect structure, electrical conductivity, and thermoelectric power. *J Solid State Chem.* 1990;87:55–63. DOI:10.1016/0022-4596(90)90064-5.
2. Ruffa AR. Thermal expansion in insulating materials. *Mater Sci.* 1980;15:2258–67. DOI:10.1007/BF00552315.
3. Ghosh K, Ogale SB, Ramesh R. Transition-element doping effects in  $\text{La}_{0.7}\text{Ca}_{0.3}\text{MnO}_3$ . *Phys Rev.* 1999;59:533–7. DOI:10.1103/PhysRevB.59.533.
4. Jia L, Gao J, Fang W. Influence of copper content on structural features and performance of pre-reduced  $\text{LaMn}_{1-x}\text{Cu}_x\text{O}_3$  ( $0\leq x<1$ ) catalysts for methanol synthesis from  $\text{CO}_2/\text{H}_2$ . *J Rare Earth.* 2010;28:747–51. DOI:10.1016/S1002-0721(09)60193-9.
5. Gallagher PK, Johnson DW, Vogel EM. Preparation, structure, and selected catalytic properties of the system  $\text{LaMn}_{1-x}\text{Cu}_x\text{O}_{3-y}$ . *J Am Ceram Soc.* 1977;60:28–31. DOI:10.1111/j.1151-2916.1977.tb16086.x.
6. Porta P, De Rossi S, Faticanti M, Minelli G, Pettiti I, Lisi L, Turco M. Perovskite-type oxides I. Structural, magnetic and morphological properties of  $\text{LaMn}_{1-x}\text{Cu}_x\text{O}_3$  and  $\text{LaCo}_{1-x}\text{Cu}_x\text{O}_3$  solid solutions with large surface area. *J Solid State Chem.* 1999;146:291–304. DOI:10.1006/jssc.1999.8326.
7. Rojas ML, Fierro JLG, Tejuca LG, Bell AT. Preparation and characterization of  $\text{LaMn}_{1-x}\text{Cu}_x\text{O}_{3+\lambda}$  perovskite oxides. *J Catal.* 1990;124:41–51. DOI:10.1016/0021-9517(90)90102-P.
8. Chan KS, Ma J, Jaenicke S, Chuah GK, Lee JY. Catalytic carbon-monoxide oxidation over strontium, cerium and copper-substituted lanthanum manganates and cobaltates. *Appl Catal A.* 1994;107:201–7. DOI:10.1016/0926-860X(94)85156-5.
9. Brown Bourzutschky JA, Homs N, Bell AT. Conversion of synthesis gas over  $\text{LaMn}_{1-x}\text{Cu}_x\text{O}_{3+\lambda}$  perovskites and related copper catalysts. *J Catal.* 1990;124:52–72. DOI:10.1016/0021-9517(90)90103-Q.

10. Tabata K, Hirano Y, Suzuki E. XPS studies on the oxygen species of  $\text{LaMn}_{1-x}\text{Cu}_x\text{O}_{3+\lambda}$ . *Appl Catal A*. 1998;170:245–54.
11. Adler SB. Factors Governing Oxygen Reduction in Solid oxide Fuel cell Cathodes. *Chem Rev*. 2004;104:4791–844. DOI:10.1021/cr020724o.
12. Jiang Z, Zhang L, Cai L, Xia C. Bismuth oxide-coated (La, Sr)  $\text{MnO}_3$  cathodes for intermediate temperature solid oxide fuel cells with ittria-stabilized zirconia electrolytes. *Electrochim Acta*. 2009;54:3059–65. DOI:10.1016/j.electacta.2008.11.067.
13. Jiang Z, Zhang L, Feng K, Xia C. Nanoscale bismuth oxide impregnated (La, Sr)  $\text{MnO}_3$  cathodes for intermediate-temperature solid oxide fuel cells. *J Power Sources*. 2008;85:40–8. DOI:10.1016/j.jpowsour.2008.07.003.
14. Kaymieva OS, Danilova VV, Morozova MV, Buyanova ES, Petrova SA. Preparation, Structure and Characteristics of Solid Solutions  $\text{La}_{1-x}\text{Bi}_x\text{Mn}_{1-y}\text{M}_y\text{O}_3$  (M = Fe, Ni, Cu). *Chem Sustainable Development*. 2016;24:135. DOI:10.15372/KhUR20160203.
15. Kaimieva OS, Danilova VV, Kruzhkov DA, Buyanova ES, Petrova SA. The solid Solutions Based on Lanthanum Manganite as the Cathod Materials for Bismuth-Containing Solid Electrolytes. *Russ J Electrochem*. 2017;53:852–8. DOI:10.1134/S1023193517080080.
16. Kaymieva OS, Morozova MV, Buyanova ES, Mikhailovskaya ZA, Petrova SA, Tarakina NV. Crystal Structure and Characterization of  $\text{La}_{1-x}\text{Bi}_x\text{MnO}_{3+\delta}$ . *ECS Trans*. 2015;68:977–85. DOI:10.1149/06801.0977ecst.
17. Wincewicz KC, Cooper JS. Taxonomies of SOFC material and manufacturing alternatives. *J Power Sources*. 2005;140:280–96. DOI:10.1016/j.jpowsour.2004.08.032.
18. West AR. Solid State Chemistry and Its Application. New York: John Wiley & Sons; 1987. 742 p.